to 2.0 mg/ml (Fig. 2). At 500 μg/ml, the maximum growth is attained in 5 days. At 800 μg/ml, there is a lag of about 5 days, after which rapid growth ensues. About 50 to 70 percent of the chlorine is released during this period, and the rest is released in another 3 or 4 days. Continued subculturing also greatly shortens the growth lag, so that the microorganisms can utilize more than 70 percent of the 2,4,5,-T (1.5 mg/ml) in about 7 days. Incubation of the resting 2,4,5-T–grown cells with 2,4,5-T and subsequent ultraviolet and gas chromatographic examination of the supernatant fluids has demonstrated a gradual loss of 2,4,5-T with appearance of newer peaks on the gas chromatograms and shifts in the absorption maxima. More than 68 percent of chloride release occurs in about 11 hours under the incubation conditions with resting cells.

Our data demonstrate the possibility of breeding, in the laboratory, specific cultures that can utilize a persistent compound such as 2,4,5-T as a sole source of carbon. Continued subculturing with higher concentrations of 2,4,5-T has resulted in a significant reduction of the growth lag (maximal growth in 5 days with 2,4,5-T at 1.5 mg/ml), and a reduction in the number of colony types (three or four, as compared to seven or eight initially). Continued subculturing may allow the emergence of a single strain, perhaps with a 2,4,5-T–degradative plasmid.

S. T. KELLOGG
D. K. CHATTERJEE
A. M. CHAKRABARTY
Department of Microbiology and Immunology, University of Illinois Medical Center, Chicago 60612

References and Notes

1. M. J. Schneider, *Persistent Poisons* (New York Academy of Sciences, New York, 1979).
2. C. Ramel, Ed., *Chlorinated Phenoxy Acids and Their Dioxins* (Swedish Natural Science Research Council, Stockholm, 1978).
3. P. J. Gehring and J. E. Betso, in *ibid.*, pp. 122–133; C. Holden, *Science* **205**, 770 (1979); W. F. Grant, *Mutat. Res.* **65**, 83 (1979); J. A. Hanify, P. Metcalf, C. L. Nobbs, K. J. Worsley, *Science* **212**, 349 (1981).
4. R. S. Horvath, *Bull. Environ. Contam. Toxicol.* **5**, 537 (1970); A. Rosenberg and M. Alexander, *J. Agric. Food Chem.* **28**, 705 (1980); *ibid.*, p. 297.
5. M. Alexander, *Science* **211**, 132 (1981).
6. D. K. Chatterjee, S. T. Kellogg, D. R. Watkins, A. M. Chakrabarty, in *Molecular Biology, Pathogenicity, and Ecology of Bacterial Plasmids*, S. Levy, R. C. Clowes, E. Koenig, Eds. (Plenum, New York, 1981), p. 519.
7. W. Reineke and H.-J. Knackmuss, *J. Bacteriol.* **142**, 467 (1980).
8. A. L. Heinaru, C. J. Duggleby, P. Broda, *Mol. Gen. Genet.* **160**, 347 (1978); S. A. Bayley, D. W. Morris, P. Broda, *Nature (London)* **280**, 338 (1979).
9. R. Farrell and A. M. Chakrabarty, in *Plasmids of Medical, Environmental and Commercial Importance*, K. N. Timmis and A. Puhler, Eds. (Elsevier/North-Holland, Amsterdam, 1979), p. 97.
10. R. H. Don and J. M. Pemberton, *J. Bacteriol.* **145**, 681 (1981).

11. Supported by NSF grants PCM79-17526 and PFR79-05499, by research grant 15-2 from the March of Dimes Birth Defects Foundation, and by contract 68-03-2936 with the Environmental Protection Agency. We thank G. D. Ward of George D. Ward and Associates, S. G. Termaath of the U.S. Air Force Engineering and Services Center, and N. P. Kolak of the Department of Environmental Conservation, state of New York, for supplying various contaminated soil samples from dump sites; we also thank D. R. Watkins and A. Venosa of the U.S. Environmental Protection Agency in Cincinnati for criticisms and interest.

1 June 1981; revised 4 August 1981

Extrinsic Microbial Degradation of the Alligator Eggshell

Abstract. *The outer, densely calcified layer of the alligator eggshell shows progressive crystal dissolution, with the production of concentrically stepped erosion craters, as incubation progresses. This dissolution is caused by the acidic metabolic by-products of nest bacteria. Extrinsic degradation serves to gradually increase the porosity and decrease the strength of the eggshell.*

Calculations to determine the gas and water conductances of any calcified vertebrate eggshell have been based on the assumption that the porosity of the latter remains constant throughout incubation (*1*). However, in considering animals *(Alligator mississippiensis)* with a long incubation period (65 days), it is difficult to equate this concept with the need to prevent dehydration of the recently laid egg and to provide efficient respiratory gas exchange for the late embryo. Moreover, if alligator eggs are artificially incubated without nesting media—as in experimental embryological investigations (*2*)—the embryos develop fairly normally but fail to hatch because of an abnormally tough eggshell. In order to investigate these phenomena, I studied the structure and chemical composition of the alligator eggshell in 396 specimens removed from eggs at daily intervals throughout the 65-day incubation period (*3*).

The alligator eggshell consists, from the surface inward, of an outer densely calcified zone (about 100 to 200 μm thick), a honeycomb zone (about 300 to 400 μm thick), and a mammillary zone (about 20 to 30 μm thick) to which is attached the eggshell membrane (about 150 to 250 μm thick) (*3*). The entire eggshell is composed of small rhombohedral crystals of calcite (Fig. 1A) interspersed with a variable amount of organic matrix. In the outer densely calcified zone there is no detectable organic matrix, and the calcite crystals are regularly stacked in vertical layers on their *a* faces (Fig. 1, A and C to J; Figs. 3 and 4) with their *c* axes at right angles to a tangent to the shell surface at any point (Fig. 1, C to J; Figs. 3 and 4). In contrast, in the honeycomb zone there is a higher percentage of organic matrix, which creates a meshwork of vesicular holes between the calcite crystals. These holes serve as interconnections with the egg contents via spaces between the mammillae and pores in the eggshell membrane. Furthermore, in the honeycomb zone, the calcite crystals are regularly stacked in horizontal layers on their *b* faces (Fig. 1, A and C to J), with their *a* axes at right angles to a tangent to the shell surface at any point.

At the time of egg laying, numerous small surface defects are present in the outer densely calcified layer, where crystals have either failed to form or been dislodged as the eggs clink together when they are deposited in the nest one after the other. As incubation proceeds, these small defects increase in size and depth to produce erosion craters with characteristic stepped concentric rings (Figs. 2 and 3). Each of these rings is one crystal high (Figs. 3 and 4) and corresponds to a layer of calcite crystals in the outer densely calcified zone (Fig. 1, C to J; Figs. 3 and 4). Numerous microorganisms are present around the surface defects and erosion craters (Fig. 2). These microorganisms produce acidic metabolites as a fermentation product of the decaying nest vegetation; and these acids in combination with carbonic acid (generated by the hydration of expired carbon dioxide) dissolve the calcite crystals in the outer densely calcified layers, enlarging the surface defects into erosion craters (Figs. 2 and 3) in much the same way that acidogenic oral bacteria decalcify tooth enamel to produce dental caries (*4*). The method of formation of the erosion craters is shown in Fig. 1, C to J. The stepped pattern of concentric rings is caused by the regular stacking of the calcite crystals (Figs. 3 and 4) and their anisotropic properties; that is, the *c* faces of the crystals dissolve faster than either the *a* or *b* faces (*5, 6*) (Fig. 1, C to J). The dissolution of the outer layers of calcite crystals is under kinetic control (Fig. 1J; Figs. 3 and 5) since the dissolved minerals can diffuse into the adjacent nesting media while the acid is replenished at the shell surface (Fig. 1J).

0036-8075/81/1204-1135$01.00/0 Copyright © 1981 AAAS

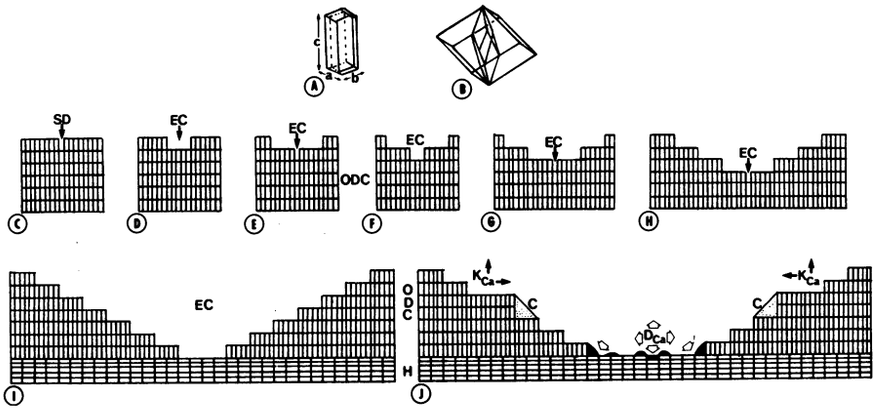

Fig. 1. (A) A habit of calcite $CaCO_3$ class 3m illustrating the general shape of the crystal and the direction of its axes *a*, *b*, and *c* [after Bunn (*5*)]. (B) A large (32-molecule) unit rhombohedron of calcite based on cleavage rhomb. The true unit cell is the small (2-molecule) steep rhombohedron shown inside [after Bunn (*5*)]. (C to J) Series of diagrams illustrating the formation of the erosion craters (*EC*) in the outer densely calcified layer (*ODC*) of the shell (here the calcite crystals are stacked in layers with their *c* axes at right angles to the shell surface). Initially, there is a surface defect (*SD*), for example, a crystal missing, and from this center acidic erosion spreads dissolving the *c* faces of the crystals more rapidly than the *a* faces. This process produces regular crater-like stepping of the calcite layers and stops at the honeycomb layer (*H*) because here the crystals are oriented with their *b* faces uppermost, and this face is more resistant to acidic erosion. In addition, the fluid at the base of the crater contains more calcium so that there is an equilibrium balance (diffusion control D_{Ca} and open arrows) with dissolution and reprecipitation of calcium (indicated by black areas), whereas near the mouth of the crater there is fluid loss so that the process is largely under kinetic control (K_{Ca} and solid arrows) with little reprecipitation. Remnants of cuticle (*C*) or other organic debris may mask layers of calcite from acid attack and so cause irregular stepping and a variety of different shapes of crater.

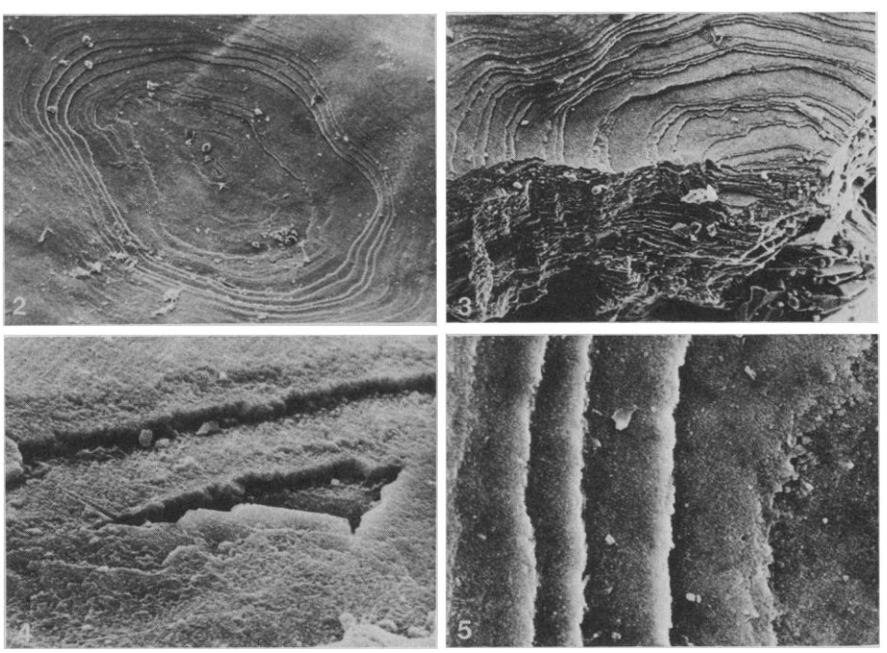

Fig. 2. Scanning electron micrograph of the surface of an alligator egg 43 days after laying. Note the regular concentrically stepped rings of the erosion crater, and the remnants of nesting debris and microorganisms. Fig. 3. Scanning electron micrograph of the surface and radially fractured (by natural cracking) edge of an erosion crater in an alligator egg 48 days after laying. The numerous layers of vertically stacked calcite crystals in the outer densely calcified zone correspond with the eroded concentric rings of the erosion crater. Fig. 4. Higher power scanning electron micrograph of the base of the erosion crater seen in Fig. 2. Each of the concentric rings of the crater is one calcite crystal high, and this corresponds with the vertical stacking of single calcite crystals (with their *a* faces one on top of the other) in the outer densely calcified zone (Fig. 3). Fig. 5. Higher power scanning electron micrograph of the concentric rings of an erosion crater in a day 48 alligator egg viewed at 90° to the shell surface. To the left are the sharp symmetrical outer rings of the erosion crater, where the dissolution of the layers of calcite crystals is under kinetic control. To the right is the basal aspect of the erosion crater where the acidic dissolution of the layers of calcite crystals is under diffusion control; here the erosion ring is neither as clearly defined nor as symmetrical as in the outer layers, and in addition it shows evidence of mineral reprecipitation (see Fig. 1).

However, remnants of cuticle or organic debris may mask certain layers of crystals, thus causing irregularities in the stepped contour (Figs. 1J and 2). The extrinsic acid eventually dissolves through all the layers of the craters' outer densely calcified zone (Fig. 1, C to J; Figs. 2, 3, and 4) but penetrates no deeper, so that the erosion craters develop broad bases on the honeycomb layer where the calcite crystals are orientated with their more resistant (to acid dissolution) *b* faces uppermost (Fig. 1, I and J). Furthermore, the dissolution of the lower layers of calcite crystals is under diffusion control (Figs. 1J, 2, and 5) as manifest by the reprecipitation of dissolved eggshell minerals and the loss of the sharp concentrically stepped edges of the erosion craters (Figs. 1J and 5). The change in orientation of the calcite crystals from the outer densely calcified zone to the honeycomb zone plus the operation of diffusion control prevent the eggshell from completely dissolving under this extrinsic acidic attack (Fig. 1J). The hypothesis that extrinsic acid is responsible for the formation of the erosion craters was tested by dripping carbonic acid (*p*H 6) onto the surface of freshly laid, pore- and crater-free eggshell fragments for 24 hours and then viewing the specimens in the scanning electron microscope. Concentrically stepped erosion craters identical to those seen in vivo (Fig. 2) are produced by this treatment. The numerous cracks that normally develop in the eggshell as incubation progresses always pass through the erosion craters (Fig. 3). The development of the erosion craters weakens the eggshell and facilitates cracking, in much the same way that it is easier to tear paper along perforations. In addition, the development of the erosion craters exposes large areas of the underlying porous honeycomb zone at the crater base (Fig. 1, I and J), which doubtlessly assist in the exchange of respiratory gases between the ever enlarging embryo and the external environment. This increasing porosity as incubation proceeds is important since no air space develops in the alligator egg while conventional pores are present only in the center of the eggshell (*3*).

The structure of the alligator eggshell is beautifully adapted to both its function and the nesting biology of the animal. Thus, at the time of laying, the eggs have a high initial strength and are not very porous, which obviously prevents damage to (and dehydration of) the eggs as they are deposited one after the other in the nest and the female treads nest vegetation on top of them. As incubation

progresses extrinsic acidic degradation of the eggshell exposes large areas of the honeycomb zone at the bases of the erosion craters, so increasing the shell porosity, which facilitates the exchange of respiratory gases and water vapor from the ever enlarging alligator embryo. The erosion craters also weaken the eggshell causing it to crack and fall off the eggshell membrane about 60 days, so facilitating hatching at 65 days. This is the first time that normal extrinsic degradation of the eggshell of any animal has been described and the first report of the ability of an eggshell to change its porosity as incubation progresses. It would be interesting to learn if the eggs of other crocodilians, which are often laid in a sandy hole as opposed to a nest of vegetation (*7*), also show this extrinsic degradation. Preliminary observations (*8*) of eggshells of *Crocodylus niloticus* (which lay their eggs in sandy holes) have shown that they exhibit erosion craters similar to those described here for *Alligator mississippiensis*. Perhaps these are formed by the action of mineral acids in the moist sand or else by acidic microbial metabolites. Further study of the microbial flora of crocodilian nests (both vegetative and sandy) and of the structure of other archosaurian eggshells is indicated. It is very important when alligator eggs are artificially incubated that they are completely surrounded by nesting medium at 28° to 30°C and 100 percent humidity. Otherwise, if nesting medium is excluded, hatching success is reduced (*9*) because the young cannot break out of the abnormally tough shell and quickly die from asphyxiation.

MARK W. J. FERGUSON
Department of Anatomy,
Queen's University of Belfast,
Belfast BT9 7BL, Northern Ireland

References and Notes

1. G. C. Packard, C. R. Tracy, J. J. Roth, *Biol. Rev.* **52**, 71 (1977); G. C. Packard, T. L. Taigen, M. J. Packard, R. D. Schuman, *Respir. Physiol.* **38**, 1 (1979).
2. M. W. J. Ferguson, *Med. Hypotheses* **5**, 1079 (1979); *Arch. Oral Biol.*, in press.
3. ———, *J. Zool.*, in press.
4. G. N. Jenkins, *The Physiology and Biochemistry of the Mouth* (Blackwell, Oxford, ed. 4, 1978).
5. C. W. Bunn, *Chemical Crystallography* (Clarendon Press, Oxford, 1945).
6. A. K. Galwey, *Chemistry of Solids* (Chapman & Hall, London, 1967); P. W. Atkins, *Physical Chemistry* (Freeman, San Francisco, 1978).
7. A. E. Greer, *Nature (London)* **227**, 523 (1970); H. W. Campbell, *ibid.* **238**, 404 (1972).
8. M. W. J. Ferguson, unpublished.
9. Louisiana Department of Wildlife and Fisheries, Grand Chenier, unpublished data.
10. Supported by Medical Research Council grant G979/386/CB and Eastern Health and Social Services Board Northern Ireland grant EB 109/74/75. I thank T. Joanen and staff, Rockefeller Wildlife Refuge, Louisiana, for help with alligator egg collection and Dr. A. Galwey for valuable discussion.

17 October 1980; revised 27 January 1981

Inhibition of Purine Nucleoside Phosphorylase by 8-Aminoguanosine: Selective Toxicity for T Lymphoblasts

Abstract. *The guanosine analog 8-aminoguanosine is an effective inhibitor of the purine degradative enzyme purine nucleoside phosphorylase, both in vitro and in intact lymphoid cells. In a human lymphoblast tissue culture system, 8-aminoguanosine, in combination with low concentrations of 2′-deoxyguanosine, causes toxicity toward T cells but not B cells. The selective T cell toxicity correlates with increased accumulation of deoxyguanosine triphosphate in the treated T lymphoblasts.*

An inhibitor of the purine degradative enzyme, purine nucleoside phosphorylase (PNP) (E.C. 2.4.2.1), has been sought because of its potential usefulness as a selective immunosuppressive agent for the treatment of certain autoimmune diseases, for the prevention of tissue rejection after organ transplantation, and for the treatment of malignant lymphoproliferative diseases. Interest in PNP as a target for pharmacologic inhibitors stems from the discovery that the hereditary deficiency of PNP is associated with severe, selective T lymphocyte dysfunction and resultant cellular immunodeficiency, without compromise of humoral immunity (*1*). The conversion of guanosine and inosine and their 2′-deoxy derivatives is catalyzed by PNP to their respective purine bases. 2′-Deoxyguanosine accumulates in the absence of PNP activity and results in a striking increase in levels of deoxyguanosine triphosphate (dGTP) in the erythrocytes of affected individuals (*2*). Similar elevations of dGTP occur in human T lymphoblasts, but not in B lymphoblasts, cultured in the presence of 2′-deoxyguanosine (*3*). The accumulation of dGTP in the T cell inhibits ribonucleotide reductase, the enzyme that catalyzes the reduction of nucleoside diphosphates to their corresponding 2′-deoxy derivatives (*4*); depletion of other deoxynucleoside triphosphates by this mechanism then results in inhibition of DNA synthesis and cell death.

Previous approaches to the selective biochemical control of immune function have focused on the use of inhibitors of adenosine deaminase (ADA) (E.C. 3.5.4.4), another enzyme in the purine catabolic pathway, which is responsible for the conversion of adenosine to inosine and deoxyadenosine to deoxyinosine. Several observations would suggest, however, that the inhibition of ADA would not be as effective or as selective in its lymphocytotoxic effect as the inhibition of PNP. While the hereditary deficiency of ADA results in T lymphocyte dysfunction and depressed cellular immunity, as does PNP deficiency, ADA-deficient patients also exhibit impairment of B lymphocyte function and associated abnormalities of humoral immunity not found with PNP deficiency (*5*). In addition, the accumulation of the ADA substrate 2′-deoxyadenosine causes not only the accumulation of deoxyadenosine triphosphate (dATP) in erythrocytes of affected individuals (*6*) as well as in immature T lymphocytes in vitro (*3*, *7*) but also inactivation of the enzyme *S*-adenosylhomocysteine hydrolase (E.C. 3.3.1.1) (*8*). The latter effect may adversely alter the function of both lymphoid and nonlymphoid cells as a consequence of *S*-adenosylhomocysteine accumulation and inhibition of *S*-adenosylmethionine–dependent methylation reactions. Indeed, the administration of deoxycoformycin, a potent inhibitor of ADA, to patients with acute lymphoblastic leukemia as well as to patients with nonhematologic malignancies produced not only a marked reduction in the numbers of both neoplastic and normal lymphoid cells but also serious toxicity involving the kidneys, lungs, and central nervous system (*9*).

These experiences with the clinical use of an ADA inhibitor have stimulated interest in the development of an inhibitor of PNP. 8-Aminoguanosine, an analog of guanosine (*10*), is the most potent PNP inhibitor discovered to date. With a K_i (inhibition constant) of 17 μM for purified erythrocyte PNP (*11*), it is six times more potent on a molar basis than formycin B, the strongest previously recognized PNP inhibitor (*12*). Thus, 8-aminoguanosine has the potential of serving as a lymphocytotoxic agent with considerable selectivity for T lymphocytes.

We have described (*3*) a cell culture system using human T and B lymphoblast cell lines with which we can reproduce the biochemical changes and selective T cell lymphocytotoxicity observed in PNP deficiency disease. In this system, a high concentration of 2′-deoxyguanosine, 50 μM, added to culture me-

0036-8075/81/1204-1137$01.00/0 Copyright © 1981 AAAS